



HAL
open science

Preliminary study for the simulation of wire ropes using a model reduction approach suitable for multiple contacts

Donald Zeka, Pierre-Alain Guidault, David Néron, Martin Guiton, Guillaume
Enchéry

► **To cite this version:**

Donald Zeka, Pierre-Alain Guidault, David Néron, Martin Guiton, Guillaume Enchéry. Preliminary study for the simulation of wire ropes using a model reduction approach suitable for multiple contacts. 25e Congrès Français de Mécanique, Aug 2022, Nantes, France. hal-03780381

HAL Id: hal-03780381

<https://hal.science/hal-03780381v1>

Submitted on 2 Jan 2024

HAL is a multi-disciplinary open access archive for the deposit and dissemination of scientific research documents, whether they are published or not. The documents may come from teaching and research institutions in France or abroad, or from public or private research centers.

L'archive ouverte pluridisciplinaire **HAL**, est destinée au dépôt et à la diffusion de documents scientifiques de niveau recherche, publiés ou non, émanant des établissements d'enseignement et de recherche français ou étrangers, des laboratoires publics ou privés.

Preliminary study for the simulation of wire ropes using a model reduction approach suitable for multiple contacts

D. ZEKA^a, P.-A. GUIDAULT^a, D. NÉRON^a, M. GUITON^b, G. ENCHERY^c

a. Université Paris-Saclay, CentraleSupélec, ENS Paris-Saclay, CNRS,
LMPS - Laboratoire de Mécanique Paris-Saclay, 91190 Gif-sur-Yvette, France
{donald.zeka, pierre-alain.guidault, david.neron}@ens-paris-saclay.fr

b. IFP Energies nouvelles, Rond-Point de l'échangeur de Solaize - BP 3, 69360 Solaize, France

c. IFP Energies nouvelles, 1-4 Avenue de Bois Préau, 92852 Rueil-Malmaison Cedex, France
{martin.guiton, guillaume.enchery}@ipfen.fr

Résumé :

Le contexte de cet article concerne la simulation de l'évolution complexe des conditions de contact et de frottement entre les fils des câbles des lignes d'ancrage d'éoliennes flottantes offshore pour prédire avec précision leur durée de vie en fatigue. Afin de faire face aux fortes non-linéarités du problème et aux temps de calcul élevés nécessaires, le solveur LATIN non linéaire et la réduction de modèle Proper Generalized Decomposition (PGD) sont proposés pour résoudre le problème. Dans ce contexte, un cas test simple unidimensionnel, représentatif du problème posé, est analysé dans le cadre LATIN-PGD : différents indicateurs de convergence pour le solveur LATIN sont étudiés afin de vérifier et assurer la convergence des quantités d'interface de contact, cruciales pour la détermination de la durée de vie en fatigue. Ensuite, la réductibilité du problème est étudiée, en se concentrant sur le tri efficace et le contrôle de la taille et de la qualité de la base réduite tout au long des itérations du solveur non linéaire.

Abstract :

The context of this paper concerns the simulation of the complex evolution of contact and friction conditions between the wires of mooring line ropes for floating offshore wind turbines to accurately predict their fatigue life. In order to deal with the strong non-linearity of the problem and the high computational times required, the non-linear LATIN solver and model-order reduction based on the Proper Generalized Decomposition (PGD) are proposed to solve the problem. In this context a one-dimensional benchmark problem, representative of the problem at hand, is analyzed within the LATIN-PGD framework: first different convergence indicators for the LATIN solver are proposed in order to check and assure convergence of local contact interface quantities, crucial for fatigue life determination. Then the reducibility of the problem is investigated, focusing on efficiently sorting and controlling the reduced basis size and quality throughout the iterations of the non-linear solver.

Keywords : Proper Generalized Decomposition, LATIN method, frictional contact.

1 Introduction

Floating offshore wind turbines (FOWTs) are basically constituted by a wind turbine installed on a floater, which is linked to the seabed by means of mooring lines, and, despite the offshore mooring technology has been used for many years, mooring line break events are still relevant concerns today. Mooring lines may be constituted by spiral strand wire ropes, which consist in a complex assembly of steel wires usually wrapped together in a twisted helical assembly of different wire layers around a single core wire. Due to their peculiar architecture, tension and bending loadings induce complex frictional phenomena between the wires that may induce fretting fatigue damage. A direct finite element analysis of the wire mechanics in order to predict fatigue life is computationally costly, since such kind of problem involves simulating the complex evolution of contact and friction conditions between the wires of the wire rope [4, 5]. In order to overcome these difficulties, reduced-order model (ROM) techniques can be used. Over the years, reduced-order models have proven themselves as reliable tools in reducing computational complexity in the context of linear and non-linear problems [12, 8]. Nevertheless, the use of reduced-order modeling can be problematic for contact problems, as a reduced-order basis may not easily and efficiently capture non-regular and propagating multiscale phenomena that occur at contact interfaces, sliding, sticking and separation zones being difficult to follow.

For contact problems, pertinent model reduction techniques rest on *a posteriori* methods. They cover POD projection-based methods for displacements and contact forces [1], adopting a non-negative matrix factorization scheme to the construction of a positive reduced basis for the contact forces. Reduced Basis methods have also been used with a greedy algorithm for the construction of a non-negative basis for the contact forces [2]. Enrichment techniques with POD modes for parametric problems have been successfully used for the simulation of fretting fatigue in [6]. In [10], the LATIN method [13] combined with a multigrid solver is applied to frictional contact problems by making use of a pre-computed reduced basis. *A priori* model reduction techniques instead rely on the Proper Generalized Decomposition (PGD) [17] and its application to contact problems with the LATIN method can be found for instance in [11, 15, 20].

The LATIN (Large Time INcrement) is a non-incremental solver for non-linear problems which iterates on the whole time-space domain [13], a peculiarity that makes it natively suitable for model-order reduction. Moreover, the resulting iterative scheme with two search directions features a robust treatment of contact non-linearities due to the fact that it shares similarities with augmented Lagrangian formulations for contact problems and Uzawa-like algorithms [23]. For the problem at hand, model reduction based on the LATIN-PGD method is exploited in this paper in order to efficiently deal with the non-linear content of the problem.

Within the target application on FOWTs, several scientific challenges arise. First of all convergence criteria for the non-linear solution method must assure a good convergence for local contact quantities: a global convergence criterion does not ensure local convergence of the interface quantities, which are crucial for fretting fatigue life prediction. Moreover, the LATIN convergence rate for contact problems strongly depends on search directions, and updating search directions is a challenging issue [25]. Another issue concerns the efficient treatment and accurate representation of the multiscale content for contact interface quantities. The use of a multiscale strategy in this case is appealing as discussed in [11] and proposed in [10]. A multiscale mixed domain decomposition method that builds a reduced basis per subdomain has been successfully proposed in [14, 15, 16, 18, 19]. In these approaches, the definition and updating of a suitable coarse problem is crucial. In this paper, the application of a domain decomposition method is not addressed but it will be revisited and studied in future works.

This paper is organized as follows: in Section 2 the LATIN method is briefly introduced along with a summary of the equations to solve at the global and the local stages in the case of a frictional contact problem. In Section 3, the LATIN method is applied on a simple one-dimensional benchmark representative of the target application, where only one frictional contact interface is considered. Various convergence and error criteria are investigated with respect to the accuracy of contact interface quantities. A study of the sensitivity of the convergence rate to the choice for the search direction is also proposed. Section 4 reports the application of PGD in order to check the reducibility of the benchmark problem following [11]. It is shown in particular how a dedicated sorting strategy for the reduced basis can improve the representation of the contact interface quantities and consequently the efficiency of the LATIN-PGD method. Conclusions and perspectives are provided in Section 5.

2 LATIN method applied to frictional contact problems

In this section the reference frictional contact problem is presented, as well as the LATIN method adopted to solve it.

2.1 Reference contact problem

Let consider, under the assumptions of small displacements and an isothermal quasi-static state, the equilibrium of a solid body occupying domain Ω over a time interval $[0, T]$ and whose boundary $\partial\Omega$ can be split into three complementary parts: $\partial_1\Omega$ where displacements \underline{u}_p are prescribed, $\partial_2\Omega$ with prescribed time-dependent external loadings $\underline{f}_{\text{ext}}$ and $\partial_3\Omega$ where contact with a rigid wall may occur (Fig. 1). Let also consider a linear elastic regime for the solid body and frictional contact conditions at the potential contact interface $\partial_3\Omega$.

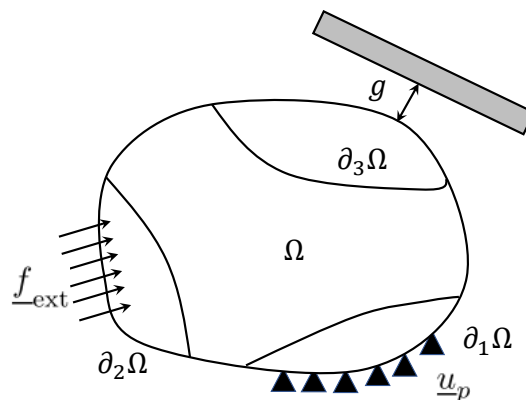


Figure 1: Frictional contact problem setting.

At the contact interface $\partial_3\Omega$, the trace of the displacement field $\underline{u}(\mathbf{x}, t)$ is $\underline{v}(\mathbf{x}, t) = \underline{u}|_{\partial_3\Omega \times [0, T]}$, and one can distinguish between normal and tangential components of displacements and contact forces $\underline{\lambda}(\mathbf{x}, t)$

with respect to $\partial_3\Omega$, as follows:

$$\forall(\mathbf{x}, t) \in \partial_3\Omega \times [0, T] : \begin{cases} \underline{v}(\mathbf{x}, t) = v_N \mathbf{n} + \underline{v}_T \\ \underline{\lambda}(\mathbf{x}, t) = \lambda_N \mathbf{n} + \underline{\lambda}_T, \end{cases} \quad (1)$$

with \mathbf{n} being the outward normal vector to $\partial\Omega$.

The problem consists in finding the displacement field $\underline{u}(\mathbf{x}, t)$ and the Cauchy's stress field satisfying kinematic admissibility, static admissibility and constitutive laws for the solid body and the contact interface. By using the finite element approximation in space for the displacement field, and by discretizing the time interval into a regular time stepping $t_{0 \leq i \leq N_t}$ such that $t_{i+1} = t_i + \Delta t$, the discretized reference frictional contact problem is to look for the vector of nodal displacements $\mathbf{u}(t)$ and contact forces $\boldsymbol{\lambda}(t)$ verifying

$$\begin{cases} \mathbf{K}\mathbf{u} = \mathbf{f}_{\text{ext}} + \mathbf{B}^T \boldsymbol{\lambda} \\ \mathcal{R}(\mathbf{v}, \boldsymbol{\lambda}) = 0 \end{cases} \quad (2)$$

for every time step, with \mathbf{K} being the stiffness matrix. The boolean matrix \mathbf{B} maps global nodal quantities to their value on the contact interface nodes, $\mathbf{v} = \mathbf{B}\mathbf{u}$ is the trace of the displacement field over the contact interface and \mathcal{R} represents the Signorini-Coulomb non-smooth constitutive law on the contact interface. Signorini conditions [22] are applied to normal contact quantities, while Coulomb frictional law [9] is used for the tangential contact behaviour.

2.2 The LATIN method

The LATIN method is a non-incremental solver for non-linear problems [13]. The main idea of the LATIN method is to separate a given problem in order to avoid the simultaneity of the global character and the non-linear (local) character of the problem. Thus, the mechanical properties of the equations are considered in order to define two manifolds: the local, and possibly non-linear, equations which belong to some non-linear manifold Γ , and the linear, and possibly global, equations which belong to some linear manifold \mathcal{A} . The search of the solution is based on a two-search direction algorithm: starting from an initial guess of the solution $\mathbf{s}_0 \in \mathcal{A}$, at each iteration a solution is alternately built in each of the manifolds as sketched in Fig. 2. The first step, called local stage, is to look for the solution $\hat{\mathbf{s}}_{n+\frac{1}{2}} \in \Gamma \cap \mathbf{E}^+$ knowing the global solution $\mathbf{s}_n \in \mathcal{A}$ at the previous iteration by making use of an ascent search direction \mathbf{E}^+ . The second step, called global stage, consists in seeking the global solution $\mathbf{s}_{n+1} \in \mathcal{A} \cap \mathbf{E}^-$ by using a descent search direction \mathbf{E}^- . The exact solution $\mathbf{s}_{\text{exact}}$ belongs to the intersection of the two manifolds. Two types of formulations can be adopted, based on the used unknowns: the formulation in displacement and the formulation in velocity. The velocity formulation is usually adopted in the context of material non-linearities, where constitutive relations are expressed in strain-rate formulation (see [16, 18, 20]), while the displacement formulation is usually more adequate in the context of linear elastic behaviour (see [6, 11]).

Here the equations to be solved for the global and the local stage for the displacement formulation of the LATIN method are summarized, where one makes use of the unknowns $\mathbf{s} = (\underline{u}, \underline{\lambda})$. The velocity formulation, based on the unknowns $\mathbf{s} = (\underline{\dot{u}}, \underline{\lambda})$, differs from the displacement formulation mainly from the fact that displacements have to be reconstructed from the velocities by making use of a pertinent time integration scheme.

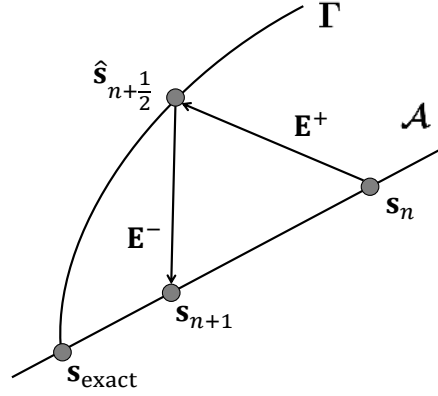


Figure 2: LATIN iteration scheme between the two manifolds.

2.2.1 Local stage

Given $\mathbf{s}_n = (\underline{u}_n, \underline{\lambda}_n) \in \mathcal{A}$ by the global stage at iteration n , the local stage is a corrective stage occurring at the contact interface and consists in finding $\hat{\mathbf{s}}_{n+\frac{1}{2}} = (\hat{\underline{u}}_{n+\frac{1}{2}}, \hat{\underline{\lambda}}_{n+\frac{1}{2}}) \in \Gamma$ by following the ascent search direction \mathbf{E}^+ :

$$(\hat{\mathbf{s}}_{n+\frac{1}{2}} - \mathbf{s}_n) \in \mathbf{E}^+ \iff \hat{\underline{\lambda}}_{n+\frac{1}{2}} - \underline{\lambda}_n = k(\hat{\underline{v}}_{n+\frac{1}{2}} - \underline{v}_n), \quad (3)$$

with k being the search direction parameter, homogeneous to a stiffness. The search direction parameter may be different from node to node and from time step to time step, it may also be updated according to the contact status; however, in the present study, a constant search direction in space and time along the iterations is adopted. The contact status on the interface can be detected by means of contact indicators C_N and C_T , defined on every contact node for the normal and tangential directions, (see [11, 6, 7] for more details). In the present work only the tangential contact is analyzed, and the definition of the tangential contact indicator is the following:

$$\mathbf{C}_T^i = \boldsymbol{\lambda}_T^i - k(\mathbf{v}_T^i - \hat{\mathbf{v}}_T^{i-1}), \quad (4)$$

where, in order to alleviate the notation, subscripts of the iterations have been removed and superscript i refers to time step t_i . At the current iteration and at the current time step, all the previous quantities are known, and, based on the value of the contact indicator, two conditions can occur, which are summarized in Tab. 1, where μ represents the friction coefficient and $\hat{\lambda}_N$ is the current value of the normal contact force at the local stage.

2.2.2 Global stage

Given the solution $\hat{\mathbf{s}}_{n+\frac{1}{2}} = (\hat{\underline{u}}_{n+\frac{1}{2}}, \hat{\underline{\lambda}}_{n+\frac{1}{2}}) \in \Gamma$ known from the previous local stage, the global stage at the current iteration consists in finding $\mathbf{s}_{n+1} = (\underline{u}_{n+1}, \underline{\lambda}_{n+1}) \in \mathcal{A}$ by following the descent search direction \mathbf{E}^- :

$$(\mathbf{s}_{n+1} - \hat{\mathbf{s}}_{n+\frac{1}{2}}) \in \mathbf{E}^- \iff \underline{\lambda}_{n+1} - \hat{\underline{\lambda}}_{n+\frac{1}{2}} = k(\hat{\underline{v}}_{n+\frac{1}{2}} - \underline{v}_{n+1}). \quad (5)$$

Local stage: tangential components	
sliding: $\ \mathbf{C}_T^i\ > \mu \hat{\lambda}_N^i $	sticking: $\ \mathbf{C}_T^i\ \leq \mu \hat{\lambda}_N^i $
$\begin{cases} \hat{\lambda}_T^i = \mu \hat{\lambda}_N^i \frac{\mathbf{C}_T^i}{\ \mathbf{C}_T^i\ } \\ \hat{\mathbf{v}}_T^i = \mathbf{v}_T^i - \frac{1}{k}(\lambda_T^i - \hat{\lambda}_T^i) \end{cases}$	$\begin{cases} \hat{\lambda}_T^i = \mathbf{C}_T^i \\ \hat{\mathbf{v}}_T^i = \mathbf{v}_T^i - \frac{1}{k}(\lambda_T^i - \hat{\lambda}_T^i) = \hat{\mathbf{v}}_T^{i-1} \end{cases}$

Table 1: Solution of the local stage for the displacement formulation of the LATIN method.

Linear constitutive law, kinematic admissibility and static admissibility have to be verified and, by taking into account the search direction (5), the following discretized problem has to be solved at the global stage for each time step t_i :

$$\begin{cases} [\mathbf{K} + \mathbf{B}^T k \mathbf{B}] \mathbf{u}^i = \mathbf{f}_{\text{ext}}^i + \mathbf{B}^T (\hat{\lambda}^i + k \hat{\mathbf{v}}^i) \\ \mathbf{v}^i = \mathbf{B} \mathbf{u}^i \\ \lambda^i = \hat{\lambda}^i + k(\hat{\mathbf{v}}^i - \mathbf{v}^i). \end{cases} \quad (6)$$

2.2.3 Initialization and error and convergence indicators

The LATIN algorithm can be initialized with the linear contactless elastic solution $\mathbf{s}_0 = (\underline{u}_0, \lambda_0) \in \mathcal{A}$ and, by denoting with $\mathbf{s}_{\text{ref}} = (\underline{u}_{\text{ref}}, \lambda_{\text{ref}})$ the reference solution of the problem, obtained with a high number of iterations of the LATIN method, one can define:

- Reference solution error:

$$\eta_{\text{ref}} = \frac{\|\mathbf{s} - \mathbf{s}_{\text{ref}}\|^2}{\|\mathbf{s}_{\text{ref}}\|^2} \quad (7)$$

- LATIN convergence indicator:

$$\eta = \frac{\|\mathbf{s} - \hat{\mathbf{s}}\|^2}{\frac{1}{2}(\|\mathbf{s}\|^2 + \|\hat{\mathbf{s}}\|^2)} \quad (8)$$

- Displacement and force convergence indicators:

$$\eta_u = \frac{\|\underline{u} - \hat{\underline{u}}\|_u^2}{\frac{1}{2}(\|\underline{u}\|_u^2 + \|\hat{\underline{u}}\|_u^2)} \quad (9)$$

$$\eta_\lambda = \frac{\|\lambda - \hat{\lambda}\|_\lambda^2}{\frac{1}{2}(\|\lambda\|_\lambda^2 + \|\hat{\lambda}\|_\lambda^2)} \quad (10)$$

- Time error indicator with respect to reference solution:

$$\eta_t = \frac{\int_{\partial_3 \Omega} [k(\underline{u}(\mathbf{x}, t) - \underline{u}_{\text{ref}}(\mathbf{x}, t))^2 + \frac{1}{k}(\lambda(\mathbf{x}, t) - \lambda_{\text{ref}}(\mathbf{x}, t))^2] dS}{\int_{\partial_3 \Omega} (k \underline{u}_{\text{ref}}^2(\mathbf{x}, t) + \frac{1}{k} \lambda_{\text{ref}}^2(\mathbf{x}, t)) dS} \quad (11)$$

with the following norms:

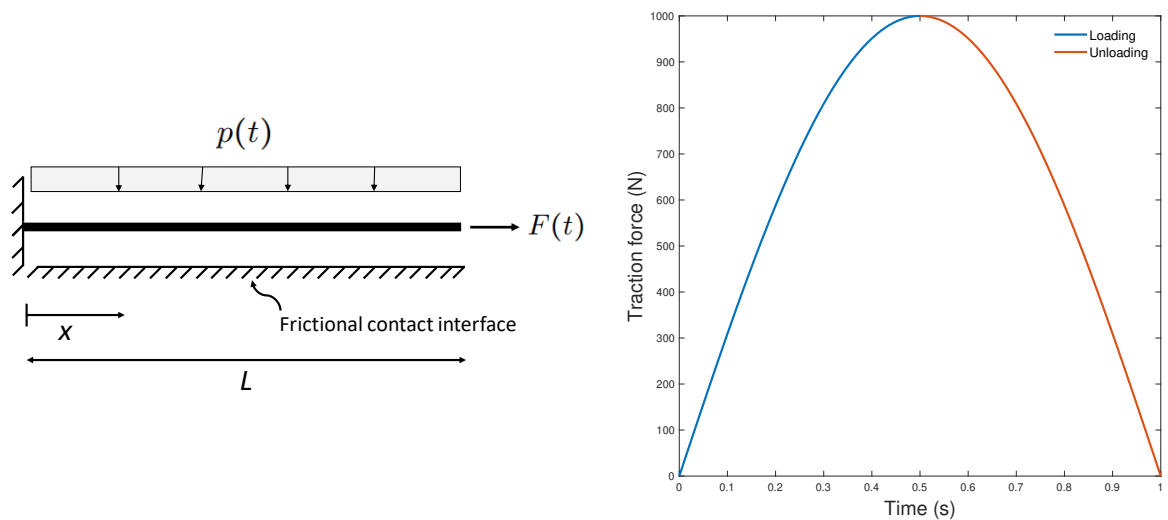
$$\|\mathbf{s}\|^2 = \int_{\partial_3\Omega} \int_{[0,T]} (k\underline{u}^2(\mathbf{x}, t) + \frac{\lambda^2(\mathbf{x}, t)}{k}) dSdt \quad (12)$$

$$\|\underline{u}\|_{\underline{u}}^2 = \int_{\partial_3\Omega} \int_{[0,T]} k\underline{u}^2(\mathbf{x}, t) dSdt \quad (13)$$

$$\|\underline{\lambda}\|_{\underline{\lambda}}^2 = \int_{\partial_3\Omega} \int_{[0,T]} \frac{1}{k} \lambda^2(\mathbf{x}, t) dSdt \quad (14)$$

3 One-dimensional numerical application

In the following section a one-dimensional benchmark problem, represented in Fig. 3a, is analyzed, that is, a one dimensional clamped bar subjected to a time dependent traction loading $F(t)$ (see Fig. 3b) and in contact with a frictional surface by means of a normal pressure $p(t)$ acting on it. The used parameters are shown in Tab. 2. In this particular case, the whole domain coincides with the contact interface (i.e., the boolean matrix \mathbf{B} reduces to the identity matrix), and the normal contact force $\underline{\lambda}_N$ is prescribed and corresponds to $p(t)$ so that only tangential behaviour has to be analyzed. The considered benchmark problem can be fairly seen as representative of the wire rope mechanics: in fact the rope is subjected to cyclic traction loadings from the sea state and, because of the helical geometry of the rope, traction and bending phenomena cause pressure loads between the different layers of wires which slide with respect to each other determining frictional contact phenomena.



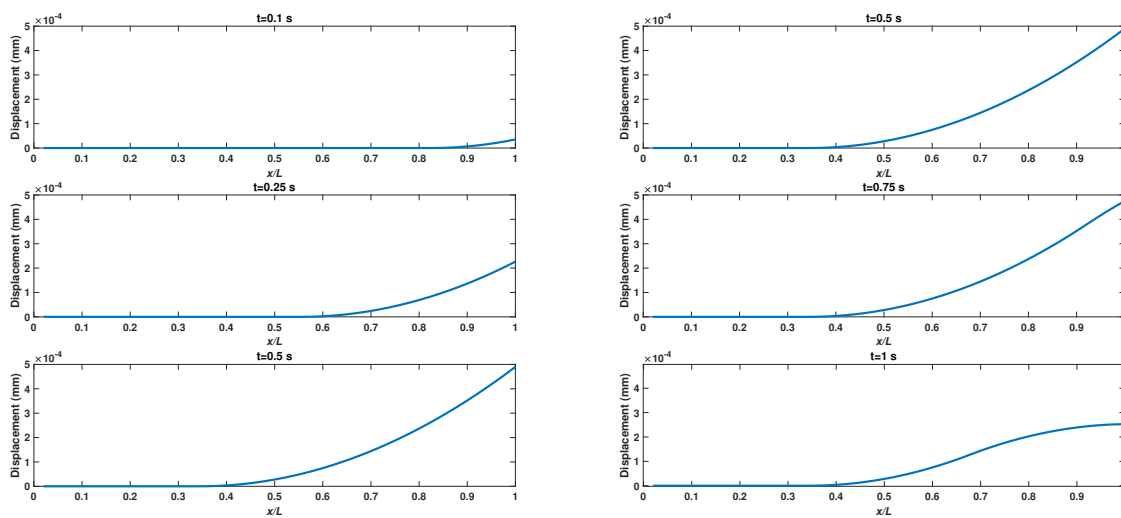
(a) One-dimensional clamped bar in contact with a frictional interface. (b) Loading and unloading stages for the traction force $F(t)$.

Figure 3: Benchmark problem set: (a) sketch of the problem, (b) time evolution of traction loading $F(t)$.

Some snapshots of the reference solution of the problem obtained with a very high number of iterations of the LATIN method (overkill solution) are shown in Fig. 4. One can notice that the sliding front propagates as the traction force increases, during the loading stage. Even during unloading, another sliding front propagates from the right top of the bar, until the traction force becomes zero, and, because of the presence of friction, the bar does not get back to its original position.

Parameters	
Young modulus, E	210 GPa
Bar cross section, S	3.14 mm ²
Bar length, L	1 m
Number of elements, N_x	50
Number of time steps, N_t	100
Time interval, T	1 s
Friction coefficient, μ	0.3
Traction force, $F(t)$	1000 $\sin(\frac{\pi t}{T})$ N
Pressure load, $p(t)$	5000 N/L

Table 2: Used parameters for the benchmark problem.

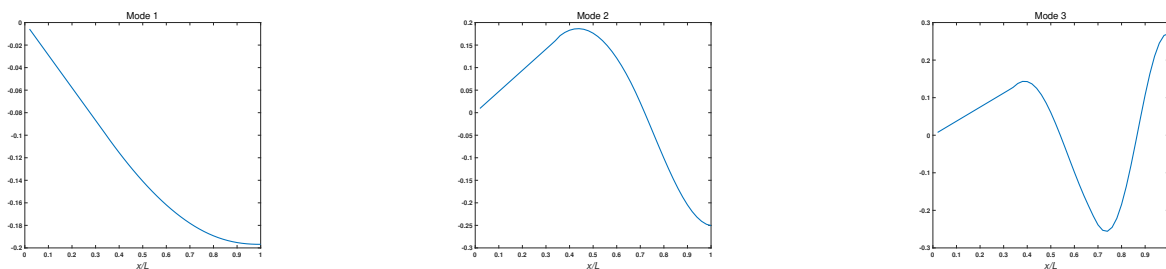


(a) Snapshots of the solution during loading.

(b) Snapshots of the solution during unloading.

Figure 4: Reference solution of the benchmark problem: (a) during loading, (b) during unloading.

Fig. 5 and Fig. 6 represent some space modes of the singular value decomposition (SVD) of the quantity $k(\mathbf{u}_{\text{ref}} - \mathbf{u}_0) + (\boldsymbol{\lambda}_{\text{ref}} - \boldsymbol{\lambda}_0)$, which will be used in the next section for the model-order reduction of the problem. We recall that the number of modes M obtained with the SVD is $M = \min(N_x, N_t) = 50$, according to Tab. 2. As found in [11], the first modes depict a global behaviour of the solution, the subsequent modes, on the other hand, bring localized corrections at specific points, which illustrates the multiscale content of frictional contact problems.

Figure 5: First three SVD space modes of $k(\mathbf{u}_{\text{ref}} - \mathbf{u}_0) + (\boldsymbol{\lambda}_{\text{ref}} - \boldsymbol{\lambda}_0)$.

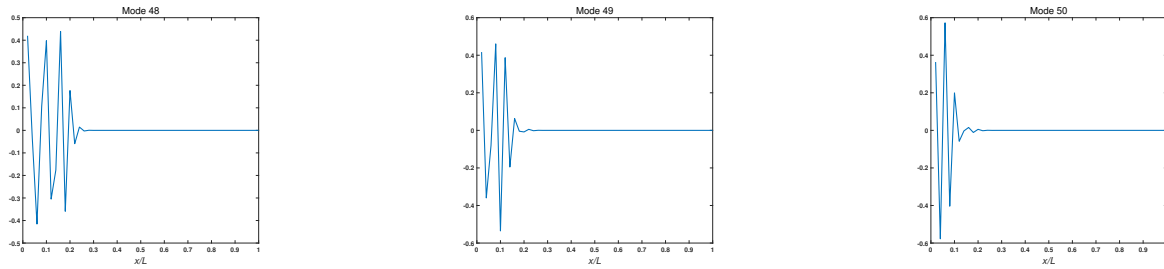


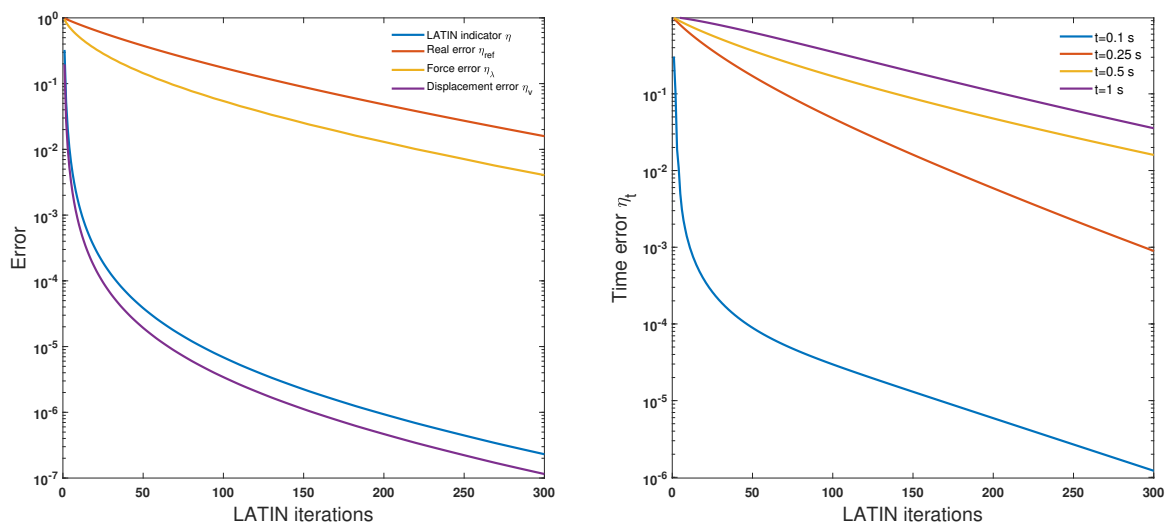
Figure 6: Last three SVD space modes of $k(\mathbf{u}_{\text{ref}} - \mathbf{u}_0) + (\boldsymbol{\lambda}_{\text{ref}} - \boldsymbol{\lambda}_0)$.

3.1 Analysis of the convergence indicators

Here the behaviour of the different error and convergence indicators defined previously in section 2.2.3 for the LATIN method are analyzed with respect to the benchmark problem. A first guess value k_0 of the search direction parameter, related to the mechanical properties of the considered problem (see [3]), has been used for this analysis, i.e.,

$$k_0 = \frac{ES}{l_{\text{el}}}, \quad (15)$$

with l_{el} being the length of the finite elements. Fig. 7 shows the evolution of the different error and convergence indicators along the iterations of the LATIN method. From Fig. 7a it can be noticed that the LATIN convergence indicator underestimates the real error for this particular problem, and, in general, one may notice that displacements converge faster than forces. Fig. 7b shows how the reference solution error behaves at different time-steps: the error presents a time propagating behaviour, at lower time steps the error is lower than the one at higher time steps.



(a) Evolution of error indicators η , η_{ref} , η_{λ} , η_{ν} along the iterations of the LATIN method.

(b) Evolution of time error η_t along the iterations of the LATIN method.

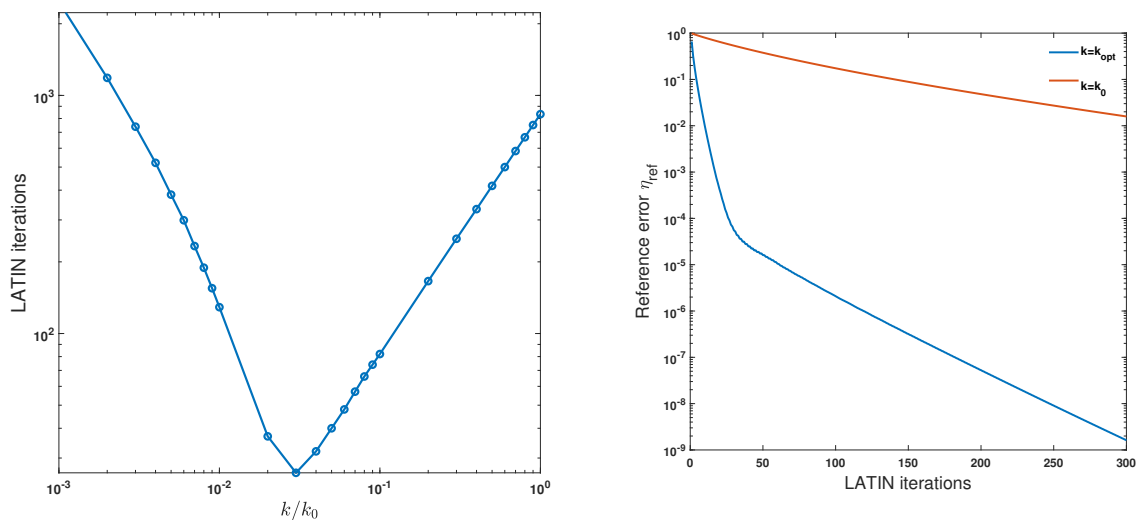
Figure 7: Error indicators for the benchmark problem with $k = k_0$: (a) global space-time errors, (b) time error η_t .

Mastering convergence behaviour is crucial for the targeted application concerning the fatigue life prediction of spiral strands: an accurate computation of local contact conditions is crucial to achieve the desired goal and, for this reason, convergence criteria must assure a good convergence of local quantities

both in space and time. As presented in this study this is a challenging issue, in fact the classical LATIN convergence indicator, which is a global indicator in space and time, may not be appropriate for our purpose since different convergence rates are observed for contact forces and displacements, as also for the different time steps. For this reason different convergence indicators can be defined, see for example [11], where a convergence indicator is defined as the maximum norm of s over all the contact nodes and all the time steps. In [20] a new convergence indicator is defined in the context of domain decomposition by taking into account the different behaviour of every interface of every subdomain (perfect interface, imposed displacement, imposed force, contact interface, etc...). These different convergence indicators will be tested in future works.

3.2 Determination of the optimal search direction

Since the LATIN method shares similarities with an augmented lagrangian formulation where the search direction parameter is analogous to the augmentation parameter, the convergence rate of the LATIN method depends on the value of the search parameter k . In the following, by considering a constant k in space and time, ones looks for the optimal value k_{opt} of search direction k which minimizes the required number of iterations to reach an error with respect to the reference solution of $\eta_{ref} = 10^{-4}$. Starting with a first guess value k_0 for the search parameter, a parametric study on the LATIN method has been performed by varying the search direction with respect to k_0 defined in Eq. (15). Fig. 8a displays the evolution of the number of iterations with respect to the search direction, and one can notice that, at least for the problem here considered, an optimal value exists and that the required number of iterations to reach convergence with this value of the search direction are far less than the reference value k_0 , as it can be seen from Fig. 8b.



(a) Evolution of the number of iterations with respect to the search direction. (b) Trend of reference error η_{ref} with $k = k_0$ and $k = k_{opt}$.

Figure 8: Parametric study on the search direction: (a) evolution of the number of iterations with respect to the search direction to reach an error level of $\eta_{ref} = 10^{-4}$, (b) reference error with $k = k_0$ and $k = k_{opt}$.

In this study it was shown how the LATIN method convergence rate is dependent on the search parameter, as for augmented lagrangian techniques [24] [25]. Here a constant value of the search direction in space and time has been adopted, however, the search parameter is related to local contact conditions at the

contact interface, i.e., sticking, sliding, contact detachment. Updating the search direction along the iterations according to the contact status on every node and every time step may be an efficient strategy to achieve a better convergence rate, and will be investigated in future works. The search parameter, however, not only affects the convergence rate of the solution but also the quality of the solution [20], for the targeted applications it is crucial to ensure, along with a fast convergence rate, also a good quality of the converged solution.

4 LATIN-PGD for frictional contact problems

The LATIN-PGD approach applied to frictional contact mechanics has been discussed in [11, 6, 20]. Here, following [11], a sorting algorithm is used to capture the best PGD modes according to the SVD. Let reformulate the global stage of the LATIN method by seeking for corrections $(\Delta \mathbf{u}, \Delta \boldsymbol{\lambda}) = (\mathbf{u}_n - \mathbf{u}_{n-1}, \boldsymbol{\lambda}_n - \boldsymbol{\lambda}_{n-1})$ between two consecutive global iterations. Given an initial linear elastic solution $\mathbf{K}\mathbf{u}_0 = \mathbf{f}_{\text{ext}}$ and $\boldsymbol{\lambda}_0 = \mathbf{0}$, the reformulated global stage of the LATIN method at the current iteration n consists in solving the following problem:

$$\begin{cases} \mathbf{K}\Delta \mathbf{u} = \mathbf{B}^T \Delta \boldsymbol{\lambda} \\ \Delta \mathbf{v} = \mathbf{B}\Delta \mathbf{u} \\ \Delta \boldsymbol{\lambda} + k\Delta \mathbf{v} - \mathbf{r}_{\text{sd}} = 0, \end{cases} \quad (16)$$

with the residual on the search direction \mathbf{r}_{sd} defined as $\mathbf{r}_{\text{sd}} = \hat{\boldsymbol{\lambda}} - \boldsymbol{\lambda}_{n-1} + k(\hat{\mathbf{v}} - \mathbf{v}_{n-1})$, known at this stage. Once the global stage is solved, displacements and contact forces are corrected accordingly. One can then introduce a space-time separated representation of both forces and displacements in the global stage of the LATIN method, that is, one looks for a separated representation of corrections $\Delta \mathbf{u} = \mathbf{V}\phi(t)$ and $\Delta \boldsymbol{\lambda} = \mathbf{L}\psi(t)$. By inserting this requirement in the equilibrium equation (16), one obtains the following condition of admissibility for space and time functions of forces and displacements:

$$\forall t \in [0, T]: \mathbf{K}\mathbf{V}\phi(t) = \mathbf{B}^T \mathbf{L}\psi(t) \iff \begin{cases} \mathbf{K}\mathbf{V} = \mathbf{B}^T \mathbf{L} \\ \phi(t) = \psi(t), \end{cases} \quad (17)$$

which means that space and time functions of forces and displacements are not independent. Problem (16), including the separated representation of corrections respecting admissibility (17), is over-constrained, as a consequence, search direction equation is verified at best in a weak sense by solving the following problem:

$$\{\mathbf{W}, \phi(t)\} = \arg \min_{\overline{\mathbf{W}}, \overline{\phi}} \|\overline{\mathbf{W}}\overline{\phi}(t) - \mathbf{r}_{\text{sd}}\|_F, \quad (18)$$

with $\mathbf{W} = \mathbf{L} + k\mathbf{B}\mathbf{V}$ being an auxiliary space mode introduced to take account of the linear relationship between \mathbf{V} and \mathbf{L} (see 17). With this separated representation the search equation is verified in a weak sense, but the constraint between space and time modes of forces and displacements exactly satisfies the admissibility conditions. Different approaches can be exploited, for example, by requiring the search direction to be exactly satisfied and the admissibility conditions to be satisfied in a weak sense; although, since the search direction is just a parameter of the problem, it is more reasonable to require it to be verified in a weak sense. Alg. 1 shows the so-called *quasi-optimal* LATIN-PGD scheme for contact problems introduced in [11]. It consists of three different stages: an updating stage for the whole set of time modes everytime a new couple is added to the basis (see [17] on how this stage is cheap to compute

and largely improves the quality of the solution), an orthonormalization stage applied to space modes every time a new couple $\{\mathbf{W}, \phi(t)\}$ is added to the basis, and a downsizing stage applied to time modes in order to reduce their redundancy after orthonormalization. For further details, the interested reader can refer to [11].

Algorithm 1: Quasi-optimal LATIN-PGD algorithm for frictional contact

Input:Tolerances: $\varepsilon, \varepsilon_1, \varepsilon_2$;Max iterations of downsizing stage: ξ_{max} ;Enrichment criterion: $0 \leq \theta \leq 1$;**Initialization:**Compute linear elastic solution: $\mathbf{K}\mathbf{u}_0 = \mathbf{f}_{ext}$, $\lambda_0 = 0$;Initialize PGD basis size: $p = 0$;**while** $\eta > \varepsilon$ **do** **Local stage:** find $(\hat{\mathbf{v}}, \hat{\lambda})$; **Updating stage:** **if** $p \geq 1$ **then** Compute search direction residual: $\mathbf{r}_{sd} = \hat{\lambda} + k\hat{\mathbf{v}} - (\lambda_0 + k\mathbf{B}\mathbf{u}_0 + \sum_{k=1}^p \mathbf{W}_k \phi_k(t))$;

Update time modes;

Update search direction residual;

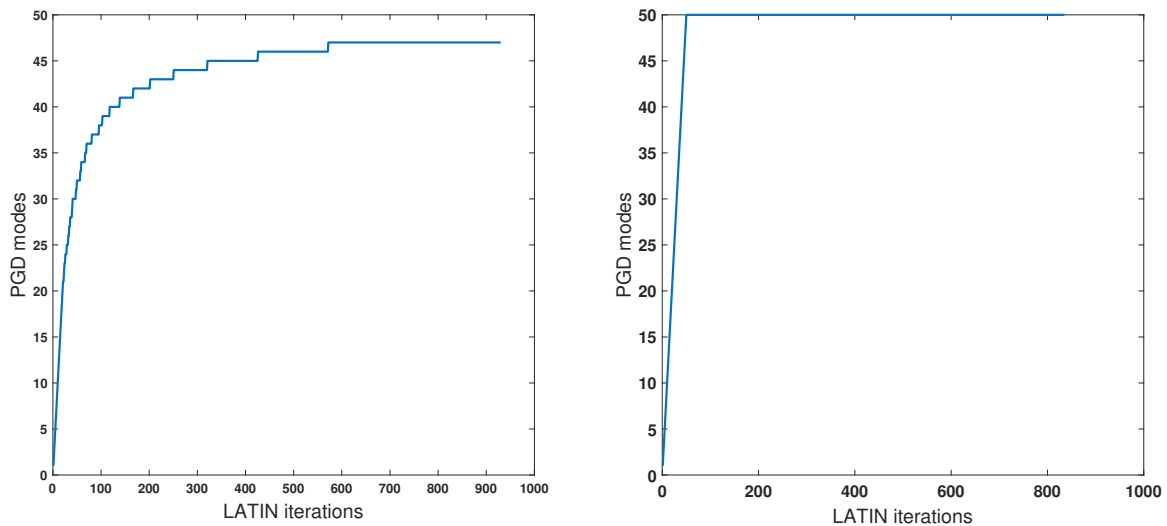
Enrichment stage with orthonormalization: **if** $1 - \eta/\eta^{old} < \theta$ **then** Find new couple $\{\mathbf{W}, \phi(t)\}$; Perform orthogonal enrichment with tolerance ε_1 : $\{\mathbf{W}, \phi(t)\} \rightarrow (\mathbf{W}_{p+1}, \phi_{p+1})$; Increment basis size: $p \leftarrow p + 1$; **Downsizing stage:** **if** $p \geq 1$ **then** Perform downsizing with iterations ξ_{max} and tolerance ε_2 ; Update basis size $q \leq p \leftarrow p$; **Convergence check:** Save previous convergence criterion $\eta^{old} \leftarrow \eta$; Compute convergence criterion η ;

The LATIN-PGD scheme illustrated in Alg. 1 is applied to the one-dimensional benchmark problem, and the effect of the different stages (updating, orthonormalization, downsizing) of the algorithm on the quality of reduced basis is analyzed. Fig. 9 and Fig. 10 show the evolution of the PGD basis along the iterations by making use of the different stages of Alg. 1. Without any additional stage, a new mode is generated at each iteration and the dimension of the PGD basis largely exceeds the dimension of the problem. This approach is not useful since modes are highly redundant and no computational saving is achieved. With orthonormalization of the space modes the dimension of the basis is controlled in size (see Fig. 9a). In fact, in the orthonormalization stage, every time a new couple is generated, the new space mode is projected onto the previously computed basis and, if the new space mode is not independent from the others, the new couple is not added to the basis according to a tolerance ε_1 . By using both orthonormalization and time function update, a full basis is generated at the first iterations (see Fig. 9b). With downsizing (see Fig. 10), one can sort and control the basis quality and size by capturing only the best PGD modes. The size of the generated basis depends on a tolerance ε_2 on the norm of the time modes. The behaviour of the PGD basis along the iterations can be easily visualized by making use of the Modal Assurance Criterion (MAC) diagrams between the PGD modes and the

SVD modes [21]. Shortly, given two sets of vectors of the same dimension $(\mathbf{X}_i)_1^p$ and $(\mathbf{Y}_i)_1^q$, the MAC matrix \mathbf{M} is defined as:

$$\mathbf{M}_{ij} = \frac{|\mathbf{X}_i^T \mathbf{Y}_j|^2}{\|\mathbf{X}_i\|^2 \|\mathbf{Y}_j\|^2} \in [0, 1]. \quad (19)$$

\mathbf{M}_{ij} measures the correlation between mode \mathbf{X}_i and mode \mathbf{Y}_j . $\mathbf{M}_{ij} = 1$ means that the modes are collinear, that is highly correlated, otherwise $\mathbf{M}_{ij} = 0$ means that the modes are orthogonal, that is highly uncorrelated.



(a) Evolution of PGD basis size with orthonormalization.

(b) Evolution of PGD basis size with orthonormalization and time functions update.

Figure 9: Evolution of PGD basis size along the iterations of the LATIN method: (a) with orthonormalization, (b) with orthonormalization and time functions update.

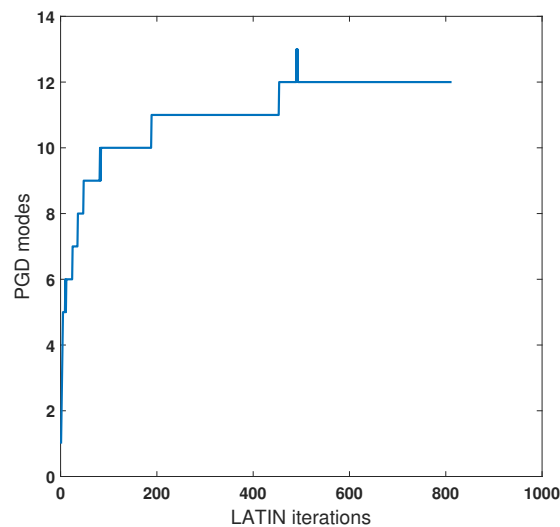


Figure 10: Evolution of PGD basis size along the iterations of the LATIN method with downsizing, orthonormalization and time function update.

Fig. 11 displays the MAC diagrams for the different stages used in the LATIN-PGD in Alg. 1. By

making use of only orthonormalization and time function update, the generated PGD modes show no correlation with the SVD. By making use also of the downsizing stage, an optimal correlation is achieved. With this sorting algorithm, it enables to capture only the best PGD modes which are closer to the SVD decomposition of the original problem.

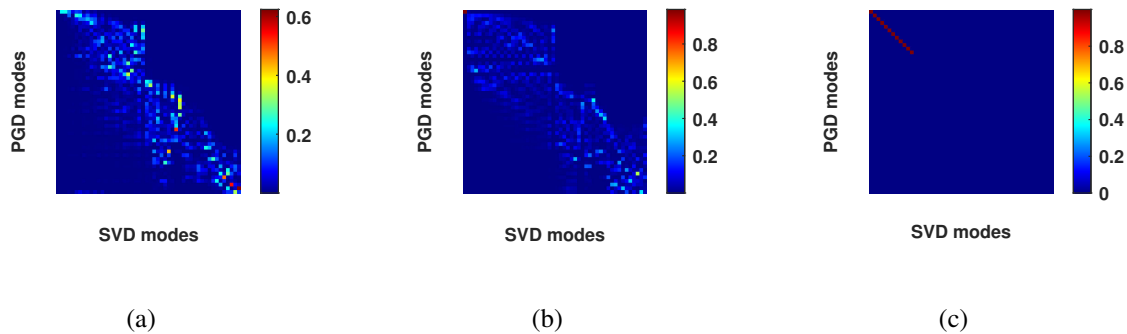


Figure 11: MAC diagrams for space modes \mathbf{W} : (a) with orthonormalization, (b) with orthonormalization and time function update, (c) with downsizing.

5 Conclusions

The reducibility of a one-dimensional frictional contact benchmark problem with the LATIN non-linear solver and the Proper Generalized Decomposition has been studied. The study on the convergence indicators shows that assuring a good convergence of local contact quantities in space and time is a challenging task: forces and displacements converge at a different rate as also convergence differs from one time step to another. Moreover the global LATIN convergence indicator can underestimate the real error with respect to the reference solution. The analysis for the search direction shows that the convergence rate of the LATIN method is highly dependent on the search direction. A well suited search direction can improve convergence and computational time. Updating the search direction based on the contact interface status can be a valuable approach that is currently being investigated. The application of PGD shows some interesting results in agreement with [11]. With the downsizing algorithm proposed in [11], the reduced basis dimension and quality can be controlled and enables to select the best (quasi-optimal) modes with the respect to the Singular Value decomposition of the problem. For future works, the multiscale version of the LATIN-based domain decomposition method [15, 16, 14, 19] will be exploited in order to introduce a coarse scale problem and to generate reduced basis per subdomain, by considering problems with multiple contact interfaces. This strategy will be revisited in order to take benefit from the multiscale content of the problem, with global and local space and time modes, while paying attention especially on the following aspects: improve convergence rate of the solution and control the quality of interface quantities, which are crucial for the target application concerning the fatigue life prediction of spiral strand wire ropes for FOWTs, with numerous and complex loadings on long time intervals.

References

- [1] M. Balajewicz, D. Amsallem, and C. Farhat. Projection-based model reduction for contact problems. *International Journal for Numerical Methods in Engineering*, 106(8):644–663, 2016.

- [2] A. Benaceur, A. Ern, and V. Ehrlacher. A reduced basis method for parametrized variational inequalities applied to contact mechanics. *International Journal for Numerical Methods in Engineering*, 121(6):1170–1197, 2020.
- [3] P.-A. Boucard and L. Champaney. A suitable computational strategy for the parametric analysis of problems with multiple contact. *International Journal for Numerical Methods in Engineering*, 57(9):1259–1281, 2003.
- [4] F. Bussolati. *Modèle multi-échelle de la fatigue des lignes d’ancrage câblées pour l’éolien offshore flottant*. PhD thesis, Université Paris-Saclay (ComUE), 2019.
- [5] F. Bussolati, P.-A. Guidault, M. Guiton, O. Allix, and P. Wriggers. *Robust contact and friction model for the fatigue estimate of a wire rope in the mooring line of a Floating Offshore Wind Turbine*, volume 93 of *Lecture Notes in Applied and Computational Mechanics*, chapter Fracture and Fatigue, pages 249–270. Springer, Cham, 2020.
- [6] A. R. Cardoso, D. Néron, S. Pommier, and J. A. Araújo. An enrichment-based approach for the simulation of fretting problems. *Computational Mechanics*, 62(6):1529–1542, 2018.
- [7] L. Champaney. *Une nouvelle approche modulaire pour l’analyse d’assemblages de structures tridimensionnelles*. PhD thesis, Ecole normale supérieure de Cachan, 1996.
- [8] F. Chinesta and P. Ladevèze. Separated representations and pgd-based model reduction. *Fundamentals and Applications, International Centre for Mechanical Sciences, Courses and Lectures*, 554:24, 2014.
- [9] C. A. Coulomb. *Théorie des machines simples en ayant égard au frottement de leurs parties et à la roideur des cordages*. Bachelier, 1821.
- [10] A. Giacomini, D. Dureisseix, A. Gravouil, and M. Rochette. A multiscale large time increment/fas algorithm with time-space model reduction for frictional contact problems. *International Journal for Numerical Methods in Engineering*, 97(3):207–230, 2014.
- [11] A. Giacomini, D. Dureisseix, A. Gravouil, and M. Rochette. Toward an optimal a priori reduced basis strategy for frictional contact problems with latin solver. *Computer Methods in Applied Mechanics and Engineering*, 283:1357 – 1381, 2015.
- [12] J. S. Hesthaven, G. Rozza, B. Stamm, et al. *Certified reduced basis methods for parametrized partial differential equations*, volume 590. Springer, 2016.
- [13] P. Ladevèze. *Nonlinear Computational Structural Mechanics - new approaches and non-incremental methods of calculation*. Mechanical Engineering Series. Springer New York, 1999.
- [14] P. Ladevèze, D. Néron, and P. Gosselet. On a mixed and multiscale domain decomposition method. *Computer Methods in Applied Mechanics and Engineering*, 196(8):1526–1540, 2007.
- [15] P. Ladevèze, A. Nouy, and O. Loiseau. A multiscale computational approach for contact problems. *Computer Methods in Applied Mechanics and Engineering*, 191(43):4869 – 4891, 2002.
- [16] P. Ladevèze, J.-C. Passieux, and D. Néron. The latin multiscale computational method and the proper generalized decomposition. *Computer Methods in Applied Mechanics and Engineering*, 199(21-22):1287–1296, 2010.

- [17] A. Nouy. A priori model reduction through proper generalized decomposition for solving time-dependent partial differential equations. *Computer Methods in Applied Mechanics and Engineering*, 199(23-24):1603–1626, 2010.
- [18] A. Nouy and P. Ladevèze. Multiscale computational strategy with time and space homogenization: A radial-type approximation technique for solving microproblems. *International Journal for Multiscale Computational Engineering*, 2(4):1543–1649, 2004.
- [19] P. Oumaziz, P. Gosselet, K. Saavedra, and N. Tardieu. Analysis, improvement and limits of the multiscale latin method. *Computer Methods in Applied Mechanics and Engineering*, 384:113955, 2021.
- [20] J.-C. Passieux. *Approximation radiale et méthode LATIN multiéchelle en temps et espace*. PhD thesis, Ecole normale supérieure de Cachan, 2008.
- [21] M. Pastor, M. Binda, and T. Harčarik. Modal assurance criterion. *Procedia Engineering*, 48:543–548, 2012.
- [22] A. Signorini. Questioni di elasticità non linearizzata e semilinearizzata. *Rendiconti di Matematica e delle sue applicazioni*, 18:95–139, 1959.
- [23] J. C. Simo and T. A. Laursen. An augmented lagrangian treatment of contact problems involving friction. *Computers & Structures*, 42(1):97–116, 1992.
- [24] D. Sun, J. Sun, and L. Zhang. The rate of convergence of the augmented lagrangian method for nonlinear semidefinite programming. *Mathematical Programming*, 114(2):349–391, 2008.
- [25] G. Zavarise and P. Wriggers. A superlinear convergent augmented lagrangian procedure for contact problems. *Engineering Computations*, 16(1):88–119, 1999.